THE JOURNAL OF BIOLOGICAL CHEMISTRY VOL. 286, NO. 11, pp. 8729–8739, March 18, 2011

Stress Chaperone GRP-78 Functions in Mineralized Matrix Formation*[S]

Received for publication, August 27, 2010, and in revised form, December 16, 2010 Published, JBC Papers in Press, January 14, 2011, DOI 10.1074/jbc.M110.179341

Sriram Ravindran[‡], Qi Gao[‡], Amsaveni Ramachandran[‡], Sylvie Blond[§], Sanda A. Predescu[¶], and Anne George[‡1]

From the Departments of [‡]Oral Biology and [§]Pharmaceutical Biotechnology, University of Illinois and the [¶]Department of Pharmacology, Rush University Medical Center, Chicago, Illinois 60612

Mineralized matrix formation is a well orchestrated event requiring several players. Glucose-regulated protein-78 (GRP-78) is an endoplasmic reticulum chaperone protein that has been implicated in functional roles ranging from involvement in cancer biology to serving as a receptor for viruses. In the present study we explored the role of GRP-78 in mineralized matrix formation. Differential expression of GRP-78 mRNA and protein was observed upon *in vitro* differentiation of primary mouse calvarial cells. An interesting observation was that GRP-78 was identified in the secretome of these cells and in the bone matrix, suggesting an extracellular function during matrix formation. *In vitro* nucleation experiments under physiological concentrations of calcium and phosphate ions indicated that GRP-78 can induce the formation of calcium phosphate polymorphs by itself, when bound to immobilized type I collagen and on demineralized collagen wafers. We provide evidence that GRP-78 can bind to DMP1 and type I collagen independent of each other in a simulated extracellular environment. Furthermore, we demonstrate the cell surface localization of GRP-78 and provide evidence that it functions as a receptor for DMP1 endocytosis in pre-osteoblasts and primary calvarial cells. Overall, this study represents a paradigm shift in the biological function of GRP-78.

GRP-78,[2] also known as hspa5, is a member of the heat shock protein 70 family. Its primary function is to act as a molecular chaperone in the endoplasmic reticulum (ER) and facilitates the proper folding and assembly of membrane and secretory proteins. However, GRP-78 has been shown to be up-regulated under stress conditions such as the presence of toxic agents (1–4). GRP-78 has been reported to be translocated to the detergent-resistant fractions of the plasma membrane of these cells (5, 6). It has also been implicated to function as a receptor for α2-macroglobulin and different viruses through lipid rafts (7–9). Interestingly, GRP-78 has been shown to possess calcium binding properties with reports of calcium binding affinity ranging from 1–2 mol of calcium/mol of GRP-78 to much larger quantities (10). The biological significance of the calcium binding ability of GRP-78 is, however, a subject of debate, with its role primarily being attributed to binding of ER Ca^{2+} similar to other sequestering proteins.

Recent studies have shown that several stress proteins play a significant role in osteoblast differentiation. Specifically, Old Astrocyte Specifically Induced Substance, an ER stress transducer, has been implicated to be involved in bone formation (11). Additionally, a study on the analysis of the secretome of differentiating human mesenchymal stem cells showed an increase in the amount of secreted stress proteins (12). This study quantitatively analyzed the presence of GRP-78 in the secreted pool of proteins and showed that the amount of secreted protein increased when the cells were subjected to *in vitro* differentiation. Increase in expression of GRP-78 was attributed to a need for protein folding as protein synthesis increased upon induction of differentiation. However, this does not explain why an increased amount of secreted GRP-78 is present in differentiating mesenchymal cells. Despite extensive studies on the function of intracellular GRP-78, the expression and function of GRP-78 in the extracellular matrix, particularly with respect to mineralized matrix formation such as bone and teeth, has not been reported.

Recently, we have demonstrated that dentin matrix protein 1 (DMP1), an acidic phosphoprotein, initially identified from the extracellular dentin matrix and implicated in differentiation of mesenchymal cells and also in biomineralization (13–23), binds to GRP-78 found on the plasma membrane of odontoblasts and is endocytosed via the caveolar pathway (24). In the present study we show that a similar physiological process occurs in pre-osteoblasts and osteoblasts. Considering the reported extracellular presence of GRP-78, its calcium binding ability, and the increase in extracellular protein levels during differentiation, we hypothesized that GRP-78 might play a regulatory role in mineralized matrix formation. We tested this hypothesis and present evidence for a novel role for GRP-78 in osteoblasts and in the formation of mineralized matrix, adding another facet to the multiple roles of this ER chaperone.

MATERIALS AND METHODS

Cell Culture—Three different cell types were used in this study. Two of them were established cell lines, namely MC3T3-E1 mouse pre-osteoblast cell line (kind gift from Dr. Renny Francheschi) and rat marrow stromal cell line (RMSC) (Tulane Cancer Centre). Both cell types were grown in α-minimal essential media supplemented with 10% FBS (MC3T3-E1)

* This work was supported, in whole or in part, by National Institutes of Health Grant DE 11657. This work was also supported by the Brodie Endowment Fund.

[S] The on-line version of this article (available at http://www.jbc.org) contains supplemental Figs. 1 and 2.

[1] To whom correspondence should be addressed. Dept. of Oral Biology, University of Illinois at Chicago, Chicago, IL 60612. Tel.: 312-413-0738; Fax: 312-996-6044; E-mail: anneg@uic.edu.

[2] The abbreviations used are: GRP-78, glucose-regulated protein-78; ER, endoplasmic reticulum; ECM, extracellular matrix; DMP1, dentin matrix protein 1; RMSC, rat marrow stromal cell line; EDX, energy dispersive x-ray; TRITC, tetramethylrhodamine isothiocyanate.

or 20% FBS (RMSC). Additionally, primary calvarial osteoblasts were obtained from 5-day-old wild type CD-1 mice according to approved UIC Animal protocol (assurance no. A3460.01) and cultured in α-minimal essential media supplemented with 20% FBS and 1% penicillin streptomycin mixture. When required, differentiation media comprising of 10 μg/ml ascorbic acid, 10 mM β-glycerophosphate, and 10 nM ascorbic acid added to growth media was used. When required, serum-free differentiation media was also used.

Expression and Purification of DMP1 and GRP-78 Recombinant Proteins—Recombinant DMP1 protein without any post-translational modifications was expressed and purified as published earlier (14). Briefly, the DMP1 cDNA was amplified from the rat tooth germ without the signal peptide and cloned into pGEX-4T-3 vector (Invitrogen) and expressed as glutathione *S*-transferase (GST) fusion proteins in BL21-DE3 cells. The fusion protein was then purified by binding to a glutathione-Sepharose column, cleaved using thrombin to remove the fusion tag, and eluted through a benzamidine-Sepharose column to remove thrombin. The recombinant full-length GRP-78 was expressed as a His-tagged protein as described by Lamb *et al.* (27). Briefly, p-His_6-GRP-78 was expressed in Bl21-DE3 bacteria. The His-tagged protein was bound to a nickel column, and the recombinant protein was eluted using 1 M imidazole. The purity of both proteins was analyzed by SDS-PAGE (polyacrylamide gel electrophoresis).

Analysis of GRP-78 mRNA and Protein Levels in Primary Calvarial Cells—Primary calvarial cells were cultured to 80% confluency in 100-mm tissue culture dishes. The medium was then changed to osteogenic differentiation media (100 μg/ml ascorbic acid, 10 mM β-glycerophosphate, and 10 mM dexamethasone added to the growth media). The cells were cultured in osteogenic medium for 7, 14, and 21 days. Cells not exposed to osteogenic medium served as controls. RNA and cytosolic proteins from the cells were isolated using TRIzol (Invitrogen) reagent and M-PER extraction kit (Pierce), respectively, according to the manufacturer's protocol. The isolated proteins were resolved on SDS-PAGE, and immunoblotting was performed with anti-GRP-78 and anti-tubulin (Sigma) antibody as described previously. Densitometric analysis was performed on the immunoblots using ImageJ software with tubulin as the normalization control. Expression of GRP-78 transcript was analyzed by quantitative real time PCR using Taqman primers. Primers for GAPDH were used in the same reaction mixture, and the data were normalized to the expression of GAPDH. The experiments were performed in triplicate. Quantitative real time PCR was also performed using the SYBR Green method to identify expression levels of type I collagen and osteocalcin at 0, 7, and 14 day time points.

To obtain secreted protein pools, MC3T3-E1 and mouse primary calvarial cells were grown to 80% confluence in their growth medium in T-75 tissue culture flasks. The medium was subsequently changed to serum-free medium for a period of 48 h. The medium, containing the secreted proteins was collected from 3 flasks, centrifuged, and dialyzed extensively against double-deionized water. The dialyzed solution was then freeze-dried and reconstituted in 500 μl of PBS. 20 μl of the protein was subjected to SDS-PAGE and transferred on to nitrocellulose membrane. Media was also collected from MC3T3-E1 cells cultured in the presence of differentiation media. For these experiments the cells were grown to complete confluence, and the medium was changed to serum-free regular media or differentiation media 48 h before completion of the specified time point. At the end of the time point, the medium was collected, and the cells were trypsinized and counted to ensure that the cell number did not vary significantly between the time points. 15 μl of the reconstituted protein samples obtained from media collected from a single flask at each time point were resolved on SDS-PAGE, and immunoblotting was performed with rabbit polyclonal anti-GRP-78 primary antibody (1/1000) and a corresponding anti-rabbit HRP-conjugated secondary antibody.

In Vitro Calcium Phosphate Nucleation—The nucleation experiment was conducted as previously published (18). Briefly, pretreated cover glass was adsorbed with protein solution containing 20 μg of recombinant GRP-78 protein in 100 μl of 25 mM sodium bicarbonate buffer and incubated overnight at 4 °C in a humidified chamber. Uncoated and 20 μg of bovine serum albumin (BSA)-coated cover glass served as controls. Additionally, cover glass was also coated with type I collagen (25 μg) as per the manufacturer's instructions and then incubated with recombinant GRP-78 at saturation concentration (obtained from the binding experiment with GRP-78 and type I collagen) at 37 °C for 1 h. Plates coated with type I collagen incubated with equivalent concentrations of BSA served as controls. Demineralized dentin wafers (a gift from Dr. Anna Bedran Russo, University of Illinois at Chicago College of Dentistry) were incubated with 150 μg of GRP-78 at 4 °C overnight. Uncoated and wafers coated with the same amount of BSA served as controls. After incubation, the samples were rinsed with double-deionized water and placed into a channel connecting two halves of an electrolyte cell, one compartment containing calcium buffer (165 mM NaCl, 10 mM HEPES, 2.5 mM $CaCl_2$, pH 7.4) and the other phosphate buffer (165 mM NaCl, 10 mM HEPES, 1 mM KH_2PO_4, pH 7.4). A small electric current of 1mA was passed through the system to facilitate even distribution of the ions on the cover glass coated with the proteins. The buffers were changed regularly to maintain a constant pH. At the end of 7 days the cover glass was removed, washed with double-deionized water, dehydrated in graded ethanol solutions, and dried with hexamethyldisilazane. The samples were then imaged using a Hitachi S-3000N variable pressure scanning electron microscope. JOEL JSM 6320F field emission scanning electron microscope was used to image the dentin wafer samples. Energy dispersive x-ray (EDX) analysis was also performed using the Hitachi S-3000N for all samples to analyze the presence of calcium and phosphorous ions.

Isolation of the ECM—MC3T3-E1 cells were grown to confluence on cover glass. Cell lysis was performed while retaining the ECM intact according to published protocols (24). The ECM was then fixed in 4% paraformaldehyde and subjected to immunostaining with anti-GRP-78 antibody.

GRP-78 and Type I Collagen Binding Solid Phase Assay—5 μg of rat tail type I collagen (BD Biosciences) was coated onto 96-well plates according to the manufacturer's protocol. The wells were subsequently blocked for 1 h at room temperature

with 5% BSA in PBS and incubated with increasing concentrations of recombinant GRP-78 protein for a period of 1 h at 37 °C. Incubation was also performed with varying amounts (20, 50, and 100 μl) of secreted proteins from MC3T3-E1 cells cultured for 21 days in growth media and differentiation media. The incubation was performed overnight at 4 °C for these samples. After incubation, the wells were washed 3 times in PBS to remove excess unbound GRP-78 and incubated with rabbit anti-GRP-78 antibody (1/2000) for 1 h at room temperature. The plate was washed 3 times in PBS and incubated with anti-rabbit HRP-conjugated secondary antibody (1/3000) for 1 h at room temperature. After washing 3 times with PBS, the plates were developed using the turbo TMB ELISA substrate (Pierce) according to the manufacturer's protocol. For GRP-78 binding experiments with DMP1, 10 μg/well DMP1 was incubated with the collagen-coated plates for 2 h at room temperature to saturate the DMP1 collagen binding. The experiment was then performed as described previously with increasing concentrations of GRP-78. The data were normalized to secondary antibody and uncoated and plain ELISA substrate negative controls.

In Vitro Binding Experiment—The *in vitro* binding of recombinant DMP1 to MC3T3 cells was carried out as published previously (25).

Endocytosis of DMP1—MC3T3-E1 cells, RMSCs, or mouse primary calvarial cells were grown on coverslips placed in 6-well tissue culture dishes in their respective growth media for at least 24 h. Before the start of the experiment, the cells were washed with PBS and then incubated with 10 μg/ml FITC-labeled DMP1 at 37 °C for 30 min. FITC labeling was carried out as published previously (25). The cells were then washed extensively, fixed, permeabilized, and mounted on glass slides using mounting media with DAPI nuclear stain (Vector Laboratories). The cells were imaged using a Zeiss LSM 510 confocal laser scanning microscope.

GRP-78 Pulldown Experiment—Membrane proteins from MC3T3-E1 cells were isolated using the MEM-per membrane protein isolation kit (Pierce). The pulldown experiments were carried out as previously published (25). Briefly, the membrane protein lysate was passed through a GST-DMP1 column. The column was washed extensively, and the bound proteins were eluted under high salt conditions, dialyzed to remove salt, lyophilized, and resolved by SDS-PAGE analysis. Immunoblotting was performed using anti-GRP-78 antibody (1/1000 dilution) and HRP-conjugated anti-rabbit secondary antibody (1/3000 Cell Signaling). Lysate passed through GST column alone served as a negative control.

Generation of Plasma Membrane Patches—Plasma membrane patches from MC3T3 cells were prepared as described previously (26). The patches were fixed in 4% paraformaldehyde and immunostained with anti-GRP-78 antibody.

Immunostaining and Confocal Microscopy—For immunostaining, MC3T3-E1 cells, primary calvarial cells RMSCs, or cover glasses with ECM proteins or plasma membrane patches were fixed (after completion of the experiment) in 4% paraformaldehyde, permeabilized, and blocked with 5% BSA in PBS for 1 h at room temperature and incubated with the indicated concentrations of the primary antibody (1:100 anti-GRP-78 antibody, 1:100 anti-DMP1 antibody, 1:75 anti-caveolin1 antibody) overnight at 4 °C. After washing 3 times with PBS, the cells were incubated for 1 h at room temperature with the appropriate secondary antibody (1:100 anti-rabbit TRITC conjugate from Sigma). All secondary antibody incubations were performed in the dark to minimize loss of fluorescent signal due to photo bleaching. The cells were then washed three times in PBS and mounted on glass slides for confocal microscopy.

GRP-78 shRNA Knockdown—Five target sequences of GRP-78 gene were tested for knockdown experiments. One sequence that was effective in silencing GRP-78 was used in this experiment. MC3T3 cells were plated onto 6-well tissue culture plates at 80% confluence and allowed to attach for 24 h. They were then transiently transfected with the GRP-78 shRNA plasmid pLKO.1 (Sigma) containing the sequence CCGGCCCTTACACTTGGTATTGAAACTCGAGTTTCAATACCAAGTGTAAGGGTTTTT using Superfect (Qiagen) transfection reagent as per the manufacturer's protocol. The 3′-UTR targeting sequence (Sigma) in the same vector was used as control. 24 h post-transfection, the cells were incubated with 10 μg/ml FITC-DMP1 for 10 min. The cells were fixed, permeabilized, and immunostained with anti-GRP-78 antibody as described previously. The cells were imaged using a Zeiss Axio Observer-D1 fluorescence microscope equipped with the appropriate filter sets to view green and red fluorescence and Axiovision imaging software. The fluorescence from the cells was quantified using the Axiovision software.

Localization of GRP-78 by Immunohistochemical Analysis—Embryonic days 13.5 (E13.5) and 15.5 (E15.5) and postnatal day 1 (P1), day 3 (P3), day 5 (P5) mouse heads and day 20 (P20) mouse jaws were sectioned along the midline and embedded in paraffin. Additionally, long bones of 4-week post-natal mice were also embedded in paraffin. Sections were cut at a thickness of 5 μm. The P20 mouse jaw samples and 4-week long bone samples were demineralized before fixation and embedding. The sections were deparaffinized with xylene and hydrated through graded ethanol. They were then incubated in 3% H_2O_2 for 30 min to quench endogenous peroxidase activity and blocked with serum in PBS (Vectastain ABC peroxidase kit) for 1 h at room temperature. Sections were then incubated overnight at 4 °C with anti-GRP-78 antibody (1/100) in PBS containing 3% BSA. Slides were then washed 4× in PBS (15 min each wash). The sections that were incubated with the primary antibodies were incubated with their biotin-conjugated or fluorescently labeled secondary antibodies and washed 4× in PBS. The fluorescently labeled sections were mounted on slides and imaged with a Zeiss Axioobserver D1 microscope equipped with appropriate filter sets and light source for fluorescence imaging. Nuclei were stained with DAPI by using a mounting medium (Vector Laboratories) containing DAPI. Other sections were incubated with peroxidase-conjugated streptavidin (Vectastain ABC peroxidase kit) and developed with the DAB kit (Vector Laboratories). All experiments were performed in accordance with approved UIC animal protocol (assurance no. A3460.01).

RESULTS

Expression of GRP-78 Transcript and Protein during Differentiation in Vitro—Expression level of GRP-78 mRNA and protein upon *in vitro* differentiation of mouse primary calvarial

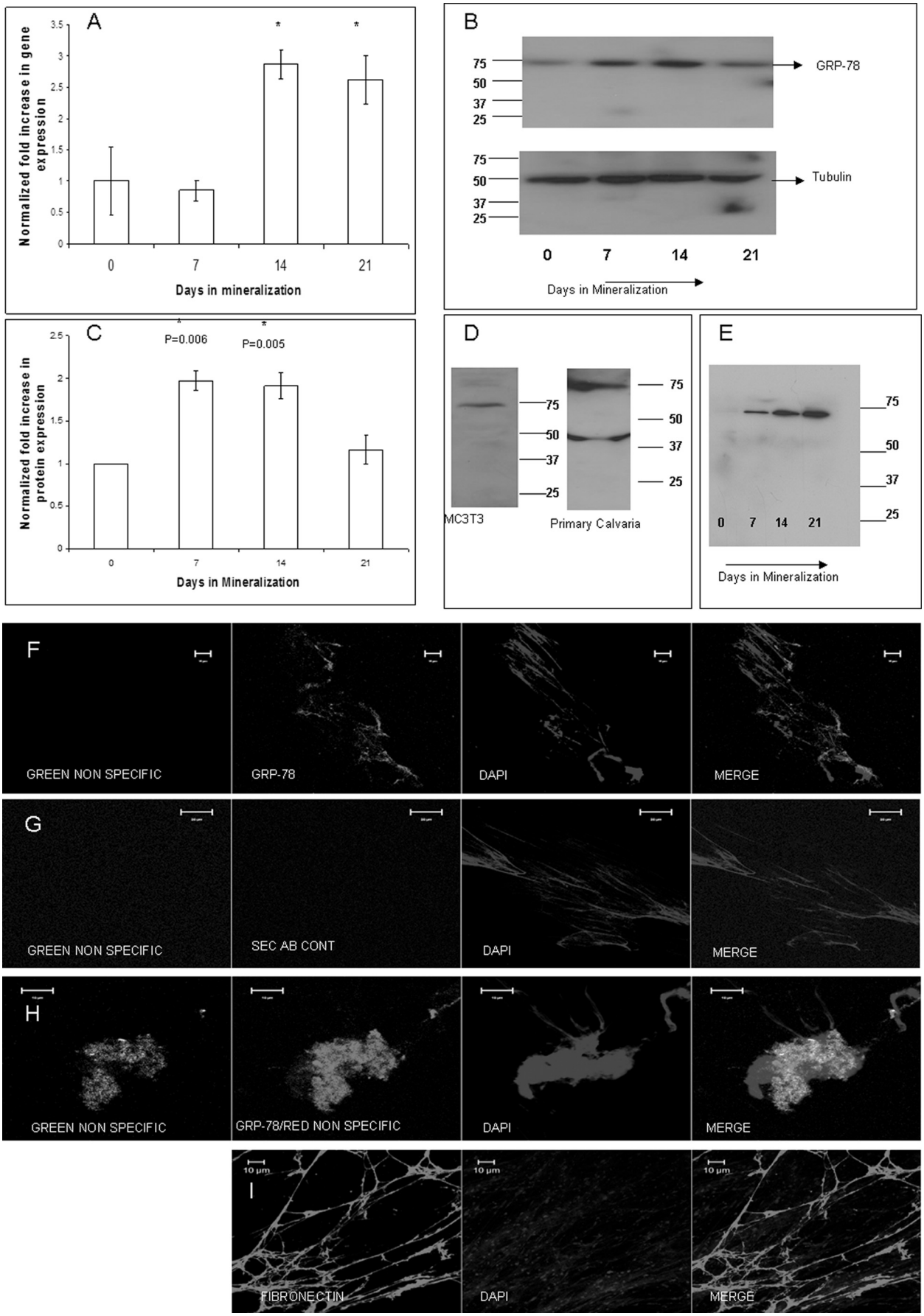
A
Normalized fold increase in gene expression
3.5
3
2.5
2
1.5
1
0.5
0
*
*
0
7
14
21
Days in mineralization
B
75
50
37
25
GRP-78
75
50
37
25
Tubulin
0
7
14
21
Days in Mineralization
C
P=0.006
P=0.005
Normalized fold increase in protein expression
2.5
2
1.5
1
0.5
0
0
7
14
21
Days in Mineralization
D
75
50
37
25
MC3T3
Primary Calvaria
E
75
50
37
25
0
7
14
21
Days in Mineralization
F
GREEN NON SPECIFIC
GRP-78
DAPI
MERGE
G
GREEN NON SPECIFIC
SEC AB CONT
DAPI
MERGE
H
GREEN NON SPECIFIC
GRP-78/RED NON SPECIFIC
DAPI
MERGE
I
10 μm
FIBRONECTIN
DAPI
MERGE

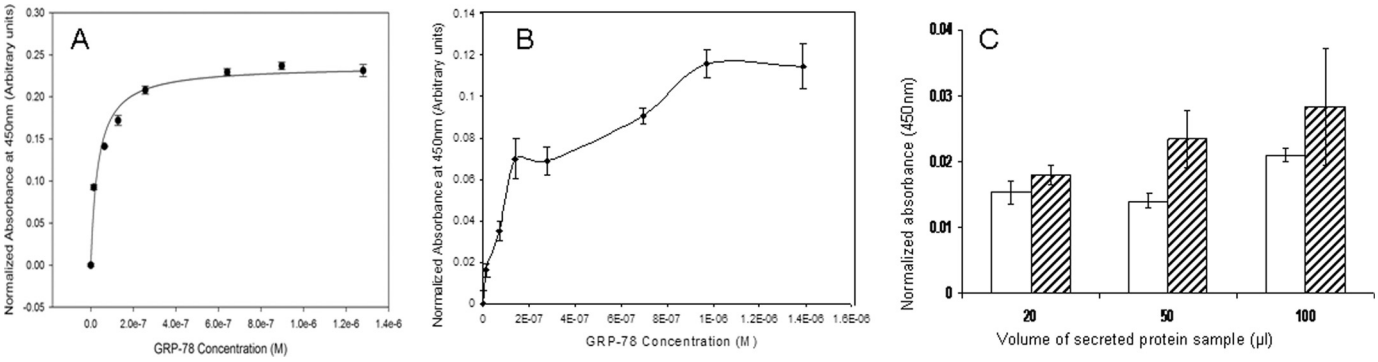

FIGURE 2. **Binding of GRP-78 to type I collagen.** *A*, shown is an inverse Langmuir isotherm plot (rectangular hyperbola) demonstrating saturable binding of GRP-78 to immobilized type I collagen. Data represent the mean ± S.E. of six experiments. The dissociation constant was estimated to be 34 nM. *B*, shown is a binding curve for binding of GRP-78 to type I collagen and DMP1 immobilized to type I collagen (DMP1 binding to type I collagen was saturated before GRP-78 binding was performed). Data represent the mean ± S.E. of six experiments. *C*, GRP-78 present in the secreted pool of proteins isolated from MC3T3 cells binds to type I collagen-coated plates. The *empty bars* represent secreted proteins from cells cultured in growth media, and the *filled bars* represent the same from cells cultured in differentiation media. Data represent the mean ± S.E. of triplicate experiments.

cells was first ascertained. Fig. 1*A* shows quantitative RT-PCR analysis of GRP-78 RNA expression in mouse primary calvarial cell cultures at 0, 7, 14. and 21 days in differentiation media. Type I collagen and osteocalcin expression were analyzed for 0, 7, and 14 days in mineralization and served as positive controls for osteogenic gene expression (supplemental Fig. 1). Fig. 1*B* shows representative immunoblots of GRP-78 intracellular protein expression and the corresponding tubulin expression in differentiating primary calvarial cultures. Fig. 1*C* is a quantification of immunoblots ($n = 4$) using the ImageJ software. An increase in the expression of RNA and protein was noted when the cells were differentiated *in vitro*.

Identification of GRP-78 in the Secretome of Preosteoblasts—To determine whether GRP-78 is a secretory protein, Western blot analysis was performed. Fig. 1*D* shows immunoblots of the total secreted proteins isolated from MC3T3-E1 and mouse primary calvarial cells that have been grown to 80% confluence without the addition of differentiation media. GRP-78 was observed in the secretome of both cell types. The secretome was also tested for the presence of tubulin to rule out contamination from dead or lysed cells. No positive tubulin band was obtained (data not shown). Therefore, GRP-78 present in the secretome is not a product of apoptotic or lysed cells in culture. Additionally, in accordance with a published report (12), GRP-78 was present in increasing amounts in the secretome of cells cultured in the presence of differentiation media (Fig. 1*E*). As the cells were grown to confluence before the addition of differentiation media, no significant change was noted in the cell number between the time points. Typically, the cell number varied between 3.8 and 4 million cells per flask between the time points. To maintain consistency in loading, the volume of media extracted from the cells, the volume of reconstitution buffer, and the loading volume were maintained constant.

Detection of GRP-78 in the ECM of MC3T3-E1 Cells—The ECM of MC3T3-E1 cells were stained with GRP-78 antibody. Fig. 1*F* shows positive staining for GRP-78. The presence of sheared DNA indicated by DAPI nuclear stain confirmed that the cells have been successfully lysed. Fig. 1*G* is a negative control showing the absence of nonspecific staining from the fluorescent secondary antibody, and Fig. 1*H* shows that the positive staining obtained in Fig. 1*F* is not due to cell debris, as the cell debris was found to fluoresce non-specifically in both red and green channels. Fig. 1*I* is a positive control that shows the presence of fibronectin in the matrix. The presence of type I collagen was also analyzed histochemically by aniline blue staining of the matrix (supplemental Fig. 2).

Binding of GRP-78 to Type I Collagen—To demonstrate a function for GRP-78 during mineralized matrix formation, a solid-phase binding assay was performed to characterize the interaction between GRP-78 and type I collagen. Results in Fig. 2*A* show the inverse Langmuir isotherm for GRP-78 binding to type I collagen. The dissociation constant was estimated to be 34 nM. The binding of GRP-78 to type I collagen was also verified in the presence of DMP1 bound to type I collagen. The rationale was to mimic the ECM environment when both DMP1 and GRP-78 are available to bind to type I collagen and to each other. The ability of DMP1 to bind to type I collagen and aid nucleation of hydroxyapatite has been shown previously (19). Results showed a two-phase binding wherein GRP-78 bound type I collagen first, as it had a higher binding affinity (comparing data from Figs. 2*A* and 7*A*) and then to the DMP1 bound to type I collagen (Fig. 2*B*). Additionally, the

FIGURE 1. **Expression of GRP-78 mRNA and protein during osteoblast differentiation.** *A*, shown is a graph representing normalized (to GAPDH) change in GRP-78 gene expression in primary calvarial cells at the indicated time points. Data represent the mean of triplicate experiments with *error bars* showing S.E. * represents p value < 0.05 as calculated by Student's t test with respect to 0-day control. *B*, immunoblots of intracellular GRP-78 and tubulin expression after 0,7,14, and 21 days in osteogenic media are shown. *C*, the graph represents change in intracellular GRP-78 protein expression in primary calvarial cells normalized to tubulin expression in the presence of differentiation media at the indicated time points. Data represent the mean of four experiments ± S.E. * represents p value < 0.05 as calculated by Student's t test with respect to 0-day control. *D*, Western blots performed with the supernatant from MC3T3-E1 cells and primary calvarial cells under non-differentiating conditions show the presence of extracellular GRP-78. *E*, an immunoblot shows the increase in extracellular GRP-78 when MC3T3-E1 cells were subjected to *in vitro* differentiation (0, 7, 14, and 21 indicate the number of days of exposure to differentiation media). *F*, GRP-78 staining in the ECM of MC3T3-E1 cells is shown. *G*, secondary antibody negative control (*SECT AB CONT*) for *F* is shown. *H*, the control shows nonspecific fluorescence observed from cell debris. *I*, a positive control shows the presence of fibronectin in the ECM of MC3T3-E1 cells.

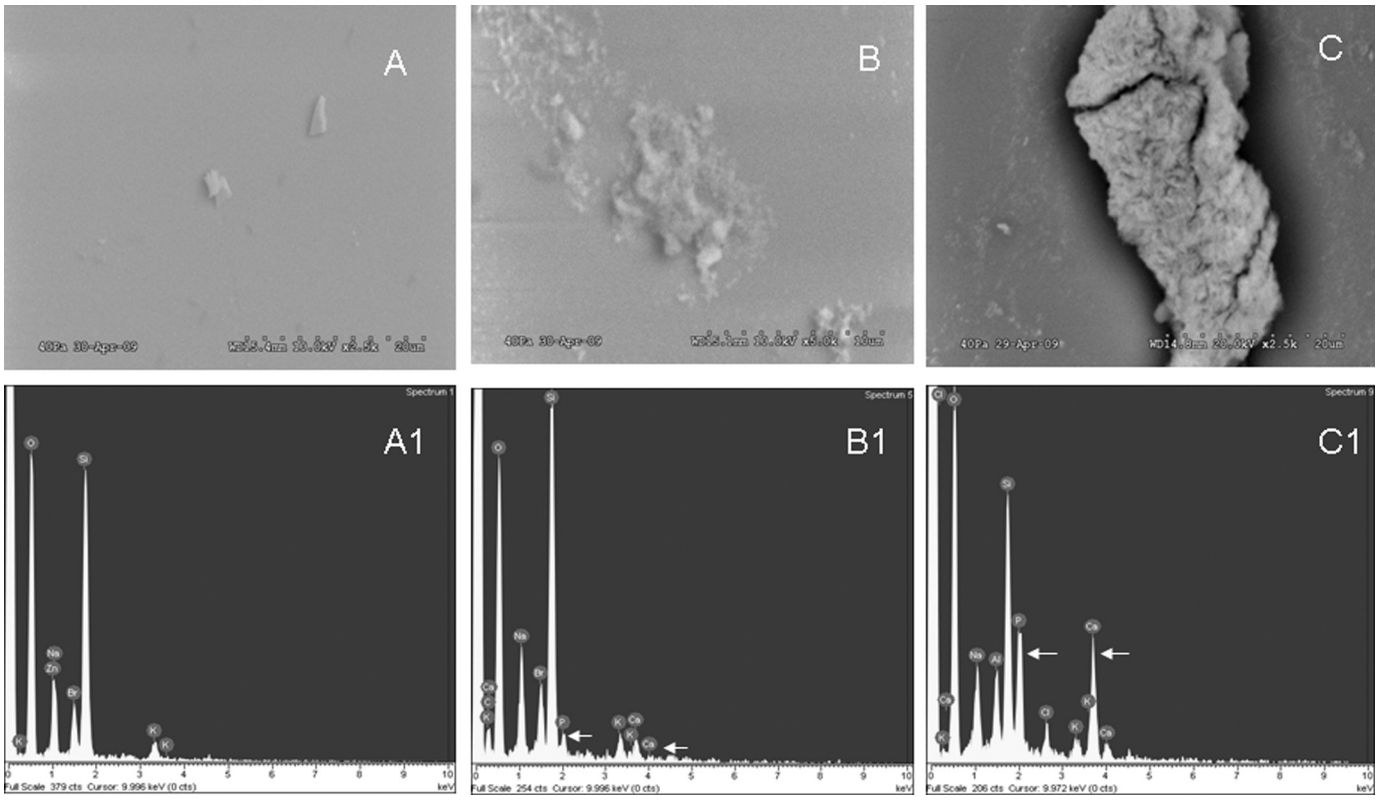

FIGURE 3. ***In vitro* nucleation of calcium phosphate by GRP-78.** *A* and *A1*, shown is an electron micrograph of control uncoated cover glass subjected to *in vitro* nucleation and its corresponding EDX analysis, respectively. The *scale bar* represents 20 μm in *A*. *B* and *B1*, shown is an electron micrograph of 20 μg of BSA-coated cover glass subjected to *in vitro* nucleation and its corresponding EDX analysis. The *scale bar* represents 10 μm in *B*. *C* and *C1*, shown is an electron micrograph of 20 μg of GRP-78-coated cover glass subjected to *in vitro* nucleation and its corresponding EDX analysis. The *scale bar* represents 20 μm in *C*. *White arrows* point to calcium and phosphorous peaks.

secreted pool of proteins from MC3T3-E1 cells, when incubated with type I collagen-coated plates showed that secreted GRP-78 was able to bind to type I collagen and that the secreted pool of proteins from mineralized cell cultures contained a higher concentration of GRP-78 (Fig. 2*C*) that can be seen by the higher amount of binding observed when compared with non-mineralizing cultures. This result shows that the native GRP-78 that is secreted out of the cell has the ability to bind to type I collagen.

In Vitro Nucleation of Calcium Phosphate Crystals by GRP-78—Published studies demonstrate that GRP-78 binds intracellular calcium (10). We investigated if immobilized GRP-78 had the potential to bind calcium and nucleate calcium phosphate crystals *in vitro*. To test this, recombinant GRP-78 immobilized on glass substrate was subjected to an *in vitro* nucleation assay. Uncoated cover glass and cover glass coated with BSA served as controls. Scanning electron microscope results in Fig. 3, *A* and *A1*, showed no calcium phosphate deposits on uncoated cover glass control. Calcium phosphate deposits were observed with BSA and GRP-78 (Fig. 3, *B* and *B1*, *C* and *C1*, respectively)-coated glass and were confirmed by EDX analysis. However, the size and the amount of calcium phosphate deposits on BSA-coated slides were far less when compared with GRP-78. The average weight percentage of calcium and phosphate ions together with respect to other elements identified by the EDX analysis for BSA-coated samples was 10.45% ($n = 3$, S.D. = 0.83), whereas GRP-78-coated substrate was 23.73% ($n = 3$, S.D. = 4.57). It should be noted that oxygen and silicon from the glass substrate made up a significant percentage. The average ratio of calcium to phosphate for BSA-coated samples was 1.45 (S.D. = 0.12), whereas the deposits for GRP-78-coated samples was 1.84 (S.D. = 0.15). We also tested the ability of type I collagen-bound GRP-78 to nucleate calcium phosphate polymorphs. Results show that type I collagen alone and type I collagen incubated with BSA did not nucleate calcium phosphate (Fig. 4, *A* and *A1*, *B* and *B1*, respectively). However, type I collagen-bound GRP-78 facilitated the deposition of calcium phosphate as confirmed by EDX analysis (Fig. 4, *C* and *C1*). The average weight percentage of calcium and phosphate together was 26.69% ($n = 3$, S.D. = 5.22), and the average Ca/P ratio was 1.88 (S.D. = 0.07). Finally, we tested the ability of GRP-78 immobilized on demineralized dentin wafers in facilitating calcium phosphate nucleation. *In vitro* mineralization experiments confirmed that GRP-78-coated dentin wafers facilitated deposition of calcium phosphate polymorphs (Fig. 5, *C* and *C1*). No nucleation was observed in uncoated and BSA-coated wafers (Fig. 5, *A* and *A1*, *B* and *B1*). The average calcium to phosphate ratio for the GRP-78 coated wafer was 1.86 ($n = 3$, S.D. = 0.22).

Developmental Expression Pattern of GRP-78—To study the developmental expression of GRP-78 protein in intramembranous and endochondral bone matrix, immunohistochemical analysis was performed. Results in Fig. 6 show strong positive staining for GRP-78 in cells producing a mineralized matrix

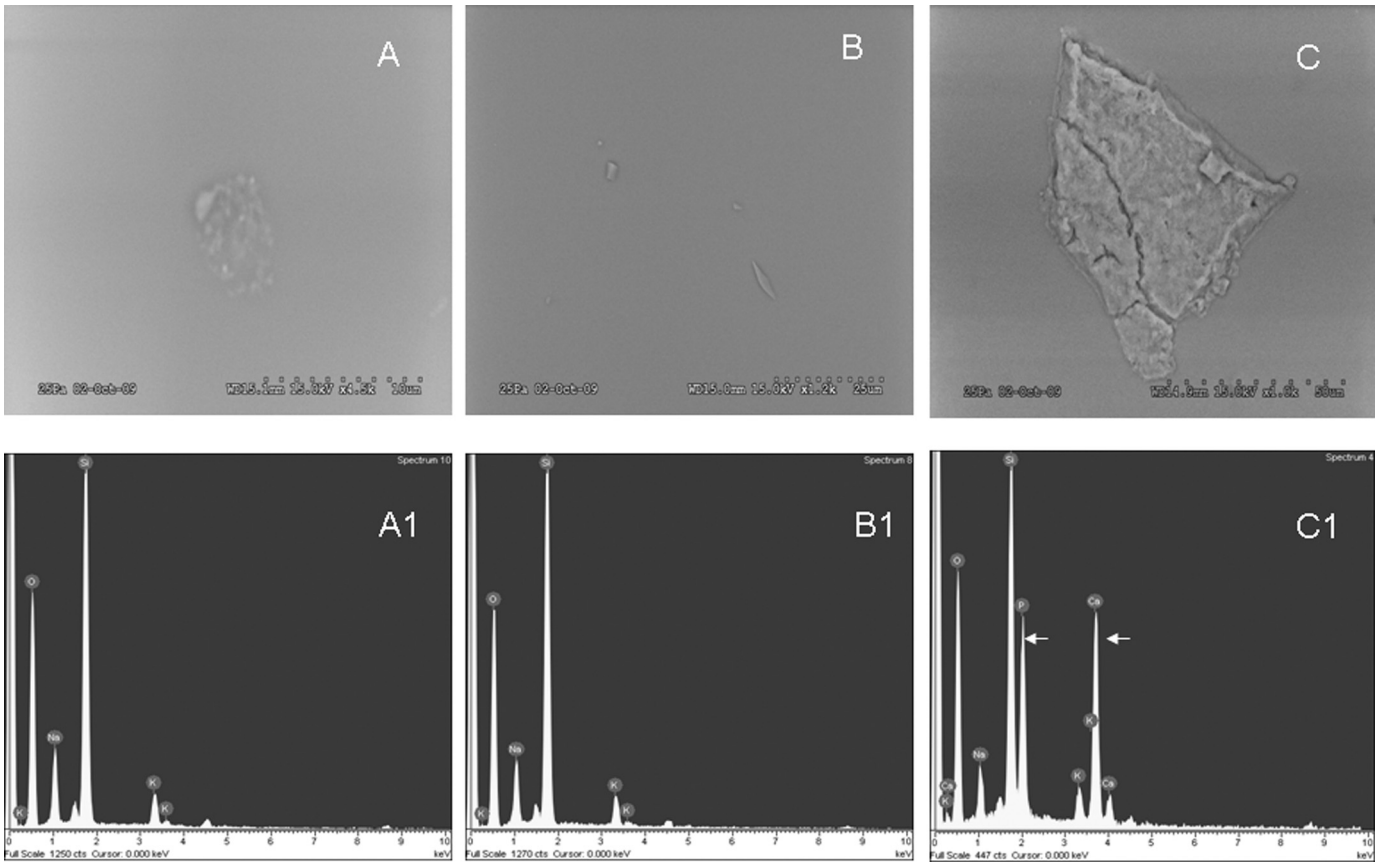

FIGURE 4. ***In vitro* nucleation of calcium phosphate by collagen bound GRP-78.** *A* and *A1*, shown is an electron micrograph of control type I collagen-coated cover glass subjected to *in vitro* nucleation and its corresponding EDX analysis, respectively. The *scale bar* represents 10 μm in *A*. *B* and *B1*, shown is an electron micrograph of BSA incubated with type I collagen-coated cover glass subjected to *in vitro* nucleation and its corresponding EDX analysis. The *scale bar* represents 25 μm in *B*. *C* and *C1*, shown is an electron micrograph of GRP-78 incubated with type I collagen-coated cover glass subjected to *in vitro* nucleation and its corresponding EDX analysis. The *scale bar* represents 50 μm in *C*. The *white arrows* point to calcium and phosphorous peaks.

(chondrocytes as well as osteocytes) (*black arrows*). The sections also showed the presence of GRP-78 in the bone matrix (*white arrows* in the peroxidase stained sections and *boxes* in the fluorescently stained sections). As expected, GRP-78 expression was observed both during early and late bone development. Fig. 6, *H*, *I*, *N*, and *O*, are secondary antibody negative controls.

Cell Surface Receptor Binds DMP1 and Facilitates Endocytosis—To elucidate DMP1 binding to the preosteoblast cell surface, we performed binding assays at 4 °C to prevent endocytosis in MC3T3-E1 cells. Fig. 7*A* shows the inverse Langmuir isotherm plot of the data from the binding experiment, demonstrating that the binding of DMP1 to MC3T3-E1 cells was saturable. The dissociation constant was estimated to be 120 nM. Thus, DMP1 binds to a cell surface receptor.

Furthermore, we demonstrate that incubating MC3T3-E1 cells at 37 °C with FITC-labeled DMP1 facilitates endocytosis (Fig. 7*B*) of DMP1. This was also observed in primary calvarial osteoblasts (Fig. 7*C*) and RMSCs (Fig. 7*D*). Longer incubation periods (45–60 min) at 37 °C resulted in nuclear translocation of the endocytosed DMP1. Fig. 7*E* shows a representative experiment with nuclear localization of endocytosed FITC-DMP1 in MC3T3-E1 cells.

GRP-78 on the Plasma Membrane Functions as a Receptor for DMP1 Endocytosis—To examine if cell surface GRP-78 functioned as a receptor mediating DMP1 endocytosis, we performed colocalization experiments. Immunostaining was performed on MC3T3-E1 cells with anti-GRP-78 antibody after endocytosis of FITC-DMP1. Fig. 8, *A* and *B*, show the co-localization of GRP-78 with DMP1 in MC3T3-E1 cells (Fig. 8*A*) as well as in primary calvarial osteoblasts (Fig. 8*B*). To elucidate the presence of GRP-78 on the plasma membrane, plasma membrane patches were prepared and immunostained with GRP-78 antibody. The *boxed region* in Fig. 8*D* shows a plasma membrane patch positively stained with GRP-78 antibody; the absence of nuclear staining compared with neighboring cells indicates an intact plasma membrane patch.

To elucidate the association of DMP1 with GRP-78 on the plasma membrane, membrane protein lysates from MC3T3-E1 cells were passed through a DMP1 column, and the bound proteins were isolated. Fig. 8*C* shows an immunoblot with anti GRP-78 antibody performed on the eluate from the column. GST beads alone did not show any reaction to GRP-78 antibody under identical experimental conditions (data not shown).

To confirm GRP-78 as a receptor for DMP1 in osteoblasts, the expression of GRP-78 was knocked down by means of shRNA in MC3T3-E1 cells. Fig. 8*E* is a graphical representation

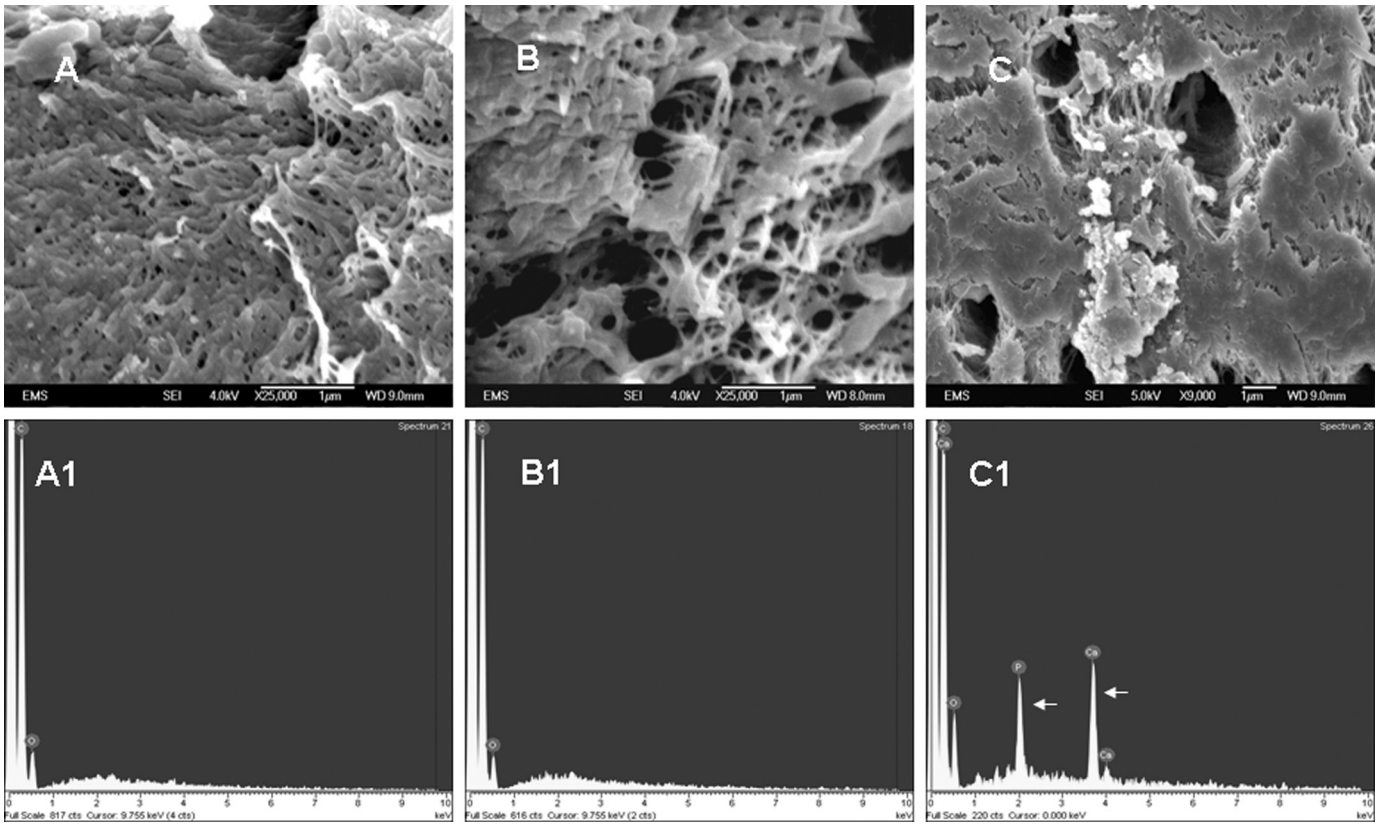

FIGURE 5. ***In vitro* nucleation of calcium phosphate by GRP-78 bound to demineralized dentin wafers.** *A* and *A1*, shown is an electron micrograph of control demineralized dentin wafers subjected to *in vitro* nucleation and EDX analysis, respectively. The *scale bar* represents 1 μm in *A*. *B* and *B1*, shown is an electron micrograph of BSA incubated with demineralized dentin wafer subjected to *in vitro* nucleation and EDX analysis. The *scale bar* represents 1 μm in *B*. *C* and *C1*, shown is an electron micrograph of GRP-78 incubated with demineralized dentin wafer subjected to *in vitro* nucleation and EDX analysis. The *scale bar* represents 1 μm in *C*. *White arrows* point to calcium and phosphorous peaks.

of FITC-DMP1 intensity and GRP-78 intensity obtained by quantification of fluorescence from cells transiently transfected with GRP-78 shRNA and subjected to FITC-DMP1 endocytosis. The intensity of endocytosed FITC-DMP1 was proportionally reduced upon GRP-78 knockdown.

Involvement of Caveolae in the Endocytic Process Mediated by GRP-78—We previously showed that endocytosis of DMP1 occurs via the caveolar endocytic pathway in odontoblasts (25). Therefore, we investigated if the same endocytic route was adopted in osteoblasts. Fig. 8*F* is a confocal micrograph that shows co-localization of endocytosed FITC-DMP1 and caveolin-1 in MC3T3-E1 cells. The *arrows* and *circled regions* in Fig. 8*F* indicate vesicles that show co-localization of FITC-DMP1 and caveolin-1. Fig. 8, *G* and *H*, are enlarged images of Fig. 8*F* that show co-localization.

DISCUSSION

GRP-78 has been shown over the years to be involved in several cellular functions apart from functioning as a molecular chaperone in the endoplasmic reticulum. GRP-78 expressed on the cell surface functions as a receptor for a wide variety of ligands and is a signaling receptor for activated α2-macroglobulin (8). It plays a critical role in viral entry of Coxsackie B and Dengue viruses (6–9). Recent studies have demonstrated GRP-78 as a secretory protein (1, 12), indicating a possible extracellular function for GRP-78. One study points to an extracellular role of GRP-78 in the zona pellucida regulating the penetration of sperm by modulating calcium ions (29). Recently, a role for extracellular GRP-78 has been identified in the regulation of inflammatory cytokines (30). Collectively, these studies indicate that GRP-78 is a multifunctional protein with a calcium binding property (10) that possesses extracellular function. In this study we demonstrate for the first time that GRP-78 is localized in the mineralizing matrix of osteoblast cultures and bone. Localization of GRP-78 in the bone matrix during development and the regulation of GRP-78 mRNA and protein expression during osteoblast differentiation indicate a functional role for GRP-78 during mineralization. When results in Fig. 1, *A* and *C*, are compared, it can be noted that at the 7-day time point, GRP-78 RNA levels are not affected, but the protein level is increased. We believe that this could be a result of translational regulation resulting in increased protein expression. Overall the data suggest that during differentiation of mesenchymal cells both transcriptional and translational regulators could play a role in modulating GRP-78 expression.

We recently showed that DMP1 is endocytosed by pre-odontoblasts and DPSCs (dental pulp stem cells) by binding to GRP-78 receptor and is translocated to the nucleus (25). Although odontoblasts and osteoblasts possess similar characteristics, differences exist between the two cell types. For example, the two cell types differ in their response to bone morphogenetic protein and TGFβ stimulation. Bone morphogenetic

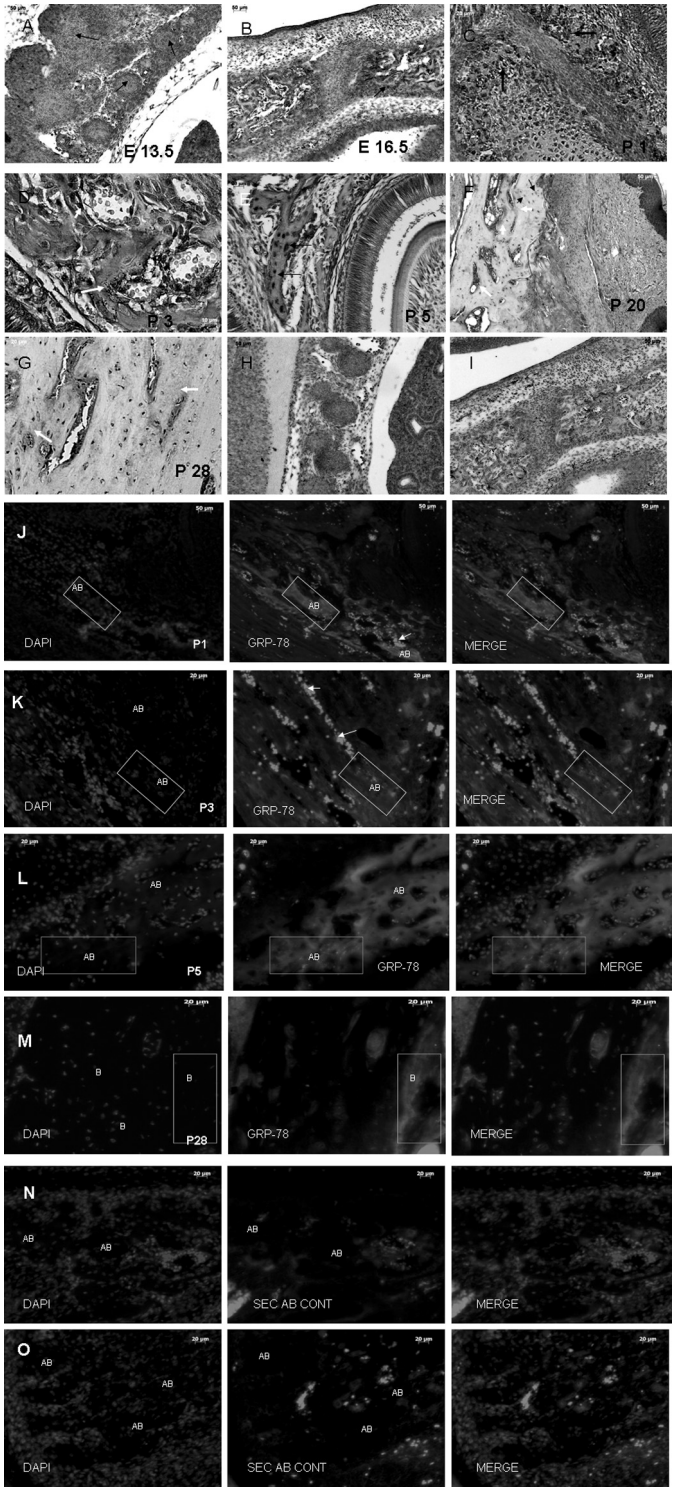

FIGURE 6. **Developmental expression pattern of GRP-78 in bone.** *A*, shown is an E13.5 whole mouse embryo immunostained with GRP-78 antibody. The *arrows* point to specific expression in chondrocytes of the vertebra. *B–E*, shown are GRP-78 immunostained sections of E16.5, P1, P3, and P5 mouse heads, respectively. *Black arrows* point to specific expression of GRP-78 in the corresponding sections. *White arrows* point to GRP-78 in the matrix. *F*, shown is P20 mouse mandible section immunostained with GRP-78 antibody. *White arrows* point to positive staining in the matrix. *G*, shown is P28 mouse long bone section immunostained with GRP-78 antibody. *White arrows* point to positive staining in the matrix. *H* and *I* are secondary antibody negative controls. *J–L*, shown is GRP-78 immunostained sections of P1, P3, and P5 mouse heads, respectively. *Boxes* mark GRP-78 localization in the matrix. *AB* represents alveolar bone. *M*, shown is the P28 mouse long bone section immunostained with GRP-78 antibody. Fluorescence shows the presence of GRP-78. The *boxed area* shows the presence of GRP-78 in the matrix. *B* represents bone. *N* and *O* represent fluorescent secondary antibody negative controls. The fluorescence seen in the control sections is due to autofluorescence from the red blood corpuscles. *AB* represents alveolar bone. Note the absence of positive staining in the alveolar bone. The *scale bar* represents 50 μm in *A*, *B*, *F*, *H*, *I*, and *J*, 20 μm in *C*, *E*, *G*, *K*, *L*, *M*, *N*, and *O*, and 10 μm in *D*.

protein/TGFβ stimulation triggers expression of RUNX2 and its target genes in osteoblasts. However, the same response in odontoblasts is triggered by fibroblast growth factor family of proteins (28). Therefore, it was necessary to study the involvement of GRP-78 in the endocytosis of DMP1 in osteoblasts. Results demonstrate that GRP-78-mediated DMP1 endocytosis is not limited to odontoblasts and occurs in preosteoblasts and osteoblasts as well. Down-regulation of GRP-78 by shRNA correspondingly reduced the amount of internalized DMP1, confirming its role in receptor-mediated endocytosis of DMP1. To determine whether endocytosis is mediated by GRP-78 localized on the cell surface, MC3T3 cell membranes were analyzed for the presence of GRP-78. Immunostaining of membrane patches confirmed cell surface localization of GRP-78. Published reports demonstrate that a subpopulation of GRP-78 exists constitutively as a transmembrane protein; therefore, it is possible that GRP-78 can be found constitutively on the cell surface of osteoblasts and pre-osteoblasts.

In addition to its role as a cell-surface receptor, we have identified GRP-78 as a secreted protein in the secretome of MC3T3-E1 cells and primary calvarial osteoblasts. We demonstrate that during *in vitro* differentiation there is an increase in the expression levels of GRP-78 in primary calvarial cells. This observation corroborates well with the published report showing expression of GRP-78 on the plasma membrane as well as in the culture medium of rabdomiosarcoma cells (1). Recently, GRP-78 has also been reported to be present in the secretome of mesenchymal stem cells, and the expression levels increased upon induction of *in vitro* differentiation for 48 h (12). In this study we observed increased secretion of GRP-78 during *in vitro* differentiation for up to 21 days. This increase in expression of the secreted protein might account for the drop in intracellular GRP-78 levels at 21 days in mineralizing calvarial cell cultures.

As GRP-78 is seen extracellularly and is also a calcium-binding protein (10), we investigated its role in the formation of mineralized matrices. We demonstrate that GRP-78 can bind to type I collagen. This was specific with a binding constant of 34 nM. In the presence of type I collagen immobilized with DMP1, we observed a two-phase binding curve. The first phase represented GRP-78 binding to type I collagen with a saturation concentration similar to that of type I collagen-GRP-78 binding by itself. The second phase is the binding of GRP-78 to DMP1 immobilized with type I collagen. This result shows that the presence of DMP1 does not alter the binding of GRP-78 to type I collagen and that GRP-78 would bind to DMP1 after saturating its type I collagen binding. It is, therefore, possible for GRP-78 in the extracellular matrix to bind to type I collagen physiologically without DMP1 competing for binding. Additionally, GRP-78 from the secreted pool of proteins was able to bind to type I collagen, con-

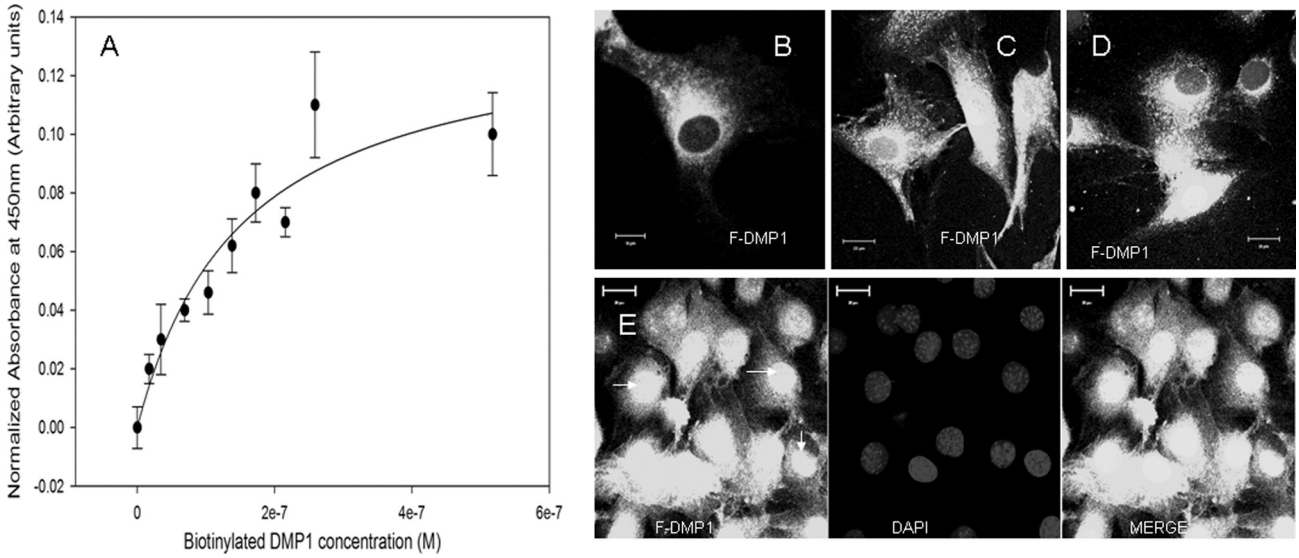

FIGURE 7. **Binding and endocytosis of DMP1.** *A*, inverse Langmuir isotherm plot (rectangular hyperbola) demonstrates saturable binding of biotinylated DMP1 to MC3T3 cells at 4 °C. Data represent the mean ± S.E. of eight experiments. The dissociation constant was estimated to be 120 nM. *B*, endocytosis of FITC-DMP1 by MC3T3 cells (*scale bar*, 10 μm) is shown. *C*, endocytosis of FITC-DMP1 by primary mouse calvarial cells (*scale bar*, 20 μm) is shown. *D*, endocytosis of FITC-DMP1 by RMSCs (*scale bar*, 20 μm) is shown. *Panel E* shows nuclear localization of the endocytosed FITC-DMP1. *Arrows* point to distinct nuclear staining of FITC-DMP1.

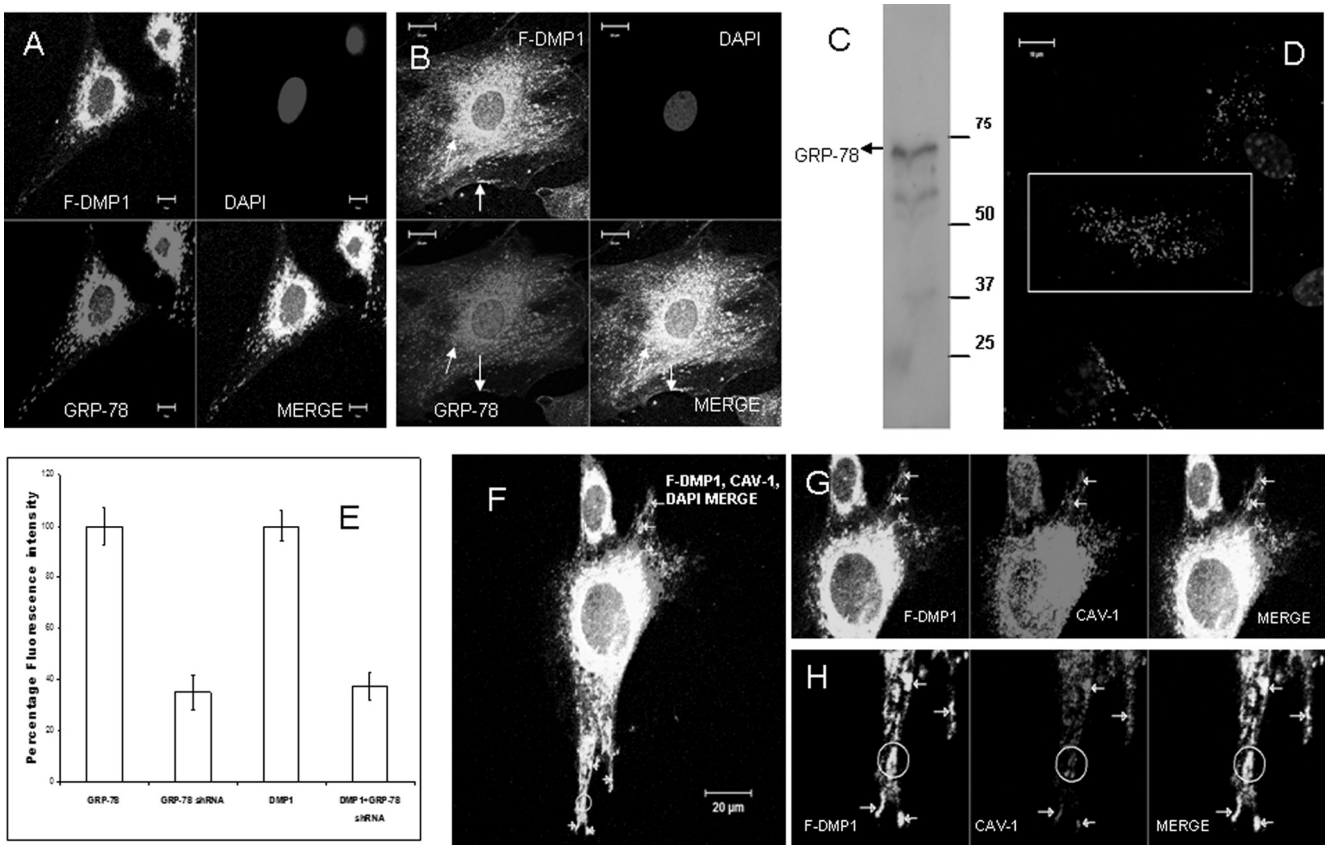

FIGURE 8. **DMP1 endocytosis; role of GRP-78 and caveolin-1.** *A* and *B*, confocal images of endocytosed FITC-DMP1 and GRP-78 in MC3T3 and primary calvarial cells, respectively, are shown. *Arrows* represent examples of colocalizing endocytic vesicles. The *scale bar* represents 10 and 20 μm, respectively. *C*, shown is a Western blot of eluate of membrane proteins bound to GST-DMP1 column with anti GRP-78 antibody. *D*, GRP-78 immunostaining of MC3T3 plasma membrane patch shows the presence of GRP-78 on the plasma membrane. *E*, quantification of fluorescence data of endocytosis of FITC-DMP1 after transient transfection with GRP-78 shRNA shows reduction in endocytosed DMP1 in GRP-78 shRNA-transfected cells. Data represent the mean ($n >= 25$ cells) ± S.E. *F*, merged confocal image of FITC-DMP1 endocytosis in MC3T3 cells immunostained with anti caveolin-1 antibody is shown. The *scale bar* represents 20 μm. *G* and *H*, enlarged images of areas from *F* show co-localizing vesicles of FITC-DMP1 and caveolin-1. *Circles* and *arrows* in all three images (*F–H*) point to co-localizing areas.

firming that the results obtained from recombinant GRP-78 are physiologically relevant. In the ER, GRP-78 has been shown to bind to pro-collagen along with other heat shock proteins (31) at the C-terminal propeptide region. Our result corroborates well with a published report that demonstrates binding of GRP-78 with gelatin (32). Collectively, it can be surmised that extracellular

GRP-78 could potentially bind to both type I collagen and to DMP1 bound to type I collagen.

In vitro nucleation experiments demonstrated that GRP-78 immobilized on a glass substrate had the potential to nucleate calcium phosphate. In bone, hydroxyapatite nucleation and growth is initiated on type I collagen scaffold. Therefore, we explored if GRP-78 immobilized on a collagen substrate or on demineralized dentin wafer would initiate calcium phosphate nucleation. Results from these experiments demonstrated that GRP-78 facilitated nucleation of amorphous calcium phosphate on a collagen template. Demineralized dentin wafers are not substitutes for demineralized bone; however, they mimic the *in vivo* type I collagen scaffold and indicate physiological relevance. During the process of biomineralization, regulation of calcium ions is of utmost importance, and their regulation by calcium-sequestering proteins in the ECM plays a central role in the nucleation of calcium phosphate. Upon analysis of our results, it is tempting to speculate that GRP-78 might function in maintaining a local reservoir of calcium ions in the ECM during mineralized matrix formation. This speculation is further strengthened by the developmental expression pattern of GRP-78 that shows increased expression in cells such as hypertrophic chondrocytes, osteoblasts, and osteocytes and also in the bone matrix.

A recent study by Murakami *et al.* has shown the involvement of the endoplasmic reticulum stress transducer Old Astrocyte Specifically Induced Substance in the formation of bone (11). This report iterates novel roles for endoplasmic reticulum stress proteins in bone formation. We believe that our finding will open new doors in understanding the multifunctional roles of these stress response proteins in calcified tissue formation.

In conclusion, the following functions for GRP-78 could be envisaged during bone formation apart from its chaperone function in the ER. 1) Extracellular GRP-78 in the matrix can specifically bind to type I collagen and/or DMP1 and sequester Ca^{2+} ions and aid in the nucleation of calcium phosphate polymorphs. 2) Cell surface GRP-78 could mediate endocytosis of DMP1 leading to subsequent signaling events. This study on the role of GRP-78 in mineralized matrix formation will unravel mechanisms that would improve our understanding on the formation of mineralized tissues such as bones and teeth.

REFERENCES

1. Delpino, A., and Castelli, M. (2002) *Biosci. Rep.* **22,** 407–420
2. Altmeyer, A., Maki, R. G., Feldweg, A. M., Heike, M., Protopopov, V. P., Masur, S. K., and Srivastava, P. K. (1996) *Int. J. Cancer* **69,** 340–349
3. Wiest, D. L., Bhandoola, A., Punt, J., Kreibich, G., McKean, D., and Singer, A. (1997) *Proc. Natl. Acad. Sci. U.S.A.* **94,** 1884–1889
4. Xiao, G., Chung, T. F., Pyun, H. Y., Fine, R. E., and Johnson, R. J. (1999) *Mol. Brain Res.* **72,** 121–128
5. Broquet, A. H., Thomas, G., Masliah, J., and Trugnan, G., Bachelet, M. (2003) *J. Biol. Chem.* **278,** 21601–21606
6. Triantafilou, K., Fradelizi, D., Wilson, K., and Triantafilou, M. (2002) *J. Virol.* **76,** 633–643
7. Triantafilou, K., and Triantafilou, M. (2003) *Virology* **317,** 128–135
8. Misra, U. K., Deedwania, R., and Pizzo, S. V. (2005) *J. Biol. Chem.* **280,** 26278–26286
9. Jindadamrongwech, S., Thepparit, C., and Smith, D. R. (2004) *Arch. Virol.* **149,** 915–927
10. Lièvremont, J. P., Rizzuto, R., Hendershot, L., and Meldolesi, J. (1997) *J. Biol. Chem.* **272,** 30873–30879
11. Murakami, T., Saito, A., Hino, S., Kondo, S., Kanemoto, S., Chihara, K., Sekiya, H., Tsumagari, K., Ochiai, K., Yoshinaga, K., Saitoh, M., Nishimura, R., Yoneda, T., Kou, I., Furuichi, T., Ikegawa, S., Ikawa, M., Okabe, M., Wanaka, A., and Imaizumi, K. (2009) *Nat. Cell Biol.* **11,** 1205–1211
12. Chiellini, C., Cochet, O., Negroni, L., Samson, M., Poggi, M., Ailhaud, G., Alessi, M. C., Dani, C., and Amri, E. Z. (2008) *BMC Mol. Biol.* **9,** 26
13. Narayanan, K., Srinivas, R., Ramachandran, A., Hao, J., Quinn, B., and George, A. (2001) *Proc. Natl. Acad. Sci. U.S.A.* **98,** 4516–4521
14. Narayanan, K., Ramachandran, A., Hao, J., He, G., Park, K. W., Cho, M., and George, A. (2003) *J. Biol. Chem.* **278,** 17500–17508
15. Narayanan, K., Gajjeraman, S., Ramachandran, A., Hao, J., and George, A. (2006) *J. Biol. Chem.* **281,** 19064–19071
16. Huang, B., Maciejewska, I., Sun, Y., Peng, T., Qin, D., Lu, Y., Bonewald, L., Butler, W. T., Feng, J., and Qin, C. (2008) *Calcif. Tissue Int.* **82,** 401–410
17. Maciejewska, I., Qin, D., Huang, B., Sun, Y., Mues, G., Svoboda, K., Bonewald, L., Butler, W. T., Feng, J. Q., and Qin, C. (2009) *Cells Tissues Organs.* **189,** 186–191
18. Lu, Y., Qin, C., Xie, Y., Bonewald, L. F., and Feng, J. Q. (2009) *Cells Tissues Organs.* **189,** 175–185
19. He, G., and George, A. (2004) *J. Biol. Chem.* **279,** 11649–11656
20. Ye, L., MacDougall, M., Zhang, S., Xie, Y., Zhang, J., Li, Z., Lu, Y., Mishina, Y., and Feng, J. Q. (2004) *J. Biol. Chem.* **279,** 19141–19148
21. Lu, Y., Ye, L., Yu, S., Zhang, S., Xie, Y., McKee, M. D., Li, Y. C., Kong, J., Eick, J. D., Dallas, S. L., and Feng, J. Q. (2007) *Dev. Biol.* **303,** 191–201
22. Ye, L., Mishina, Y., Chen, D., Huang, H., Dallas, S. L., Dallas, M. R., Sivakumar, P., Kunieda, T., Tsutsui, T. W., Boskey, A., Bonewald, L. F., and Feng, J. Q. (2005) *J. Biol. Chem.* **280,** 6197–6203
23. Feng, J. Q., Ward, L. M., Liu, S., Lu, Y., Xie, Y., Yuan, B., Yu, X., Rauch, F., Davis, S. I., Zhang, S., Rios, H., Drezner, M. K., Quarles, L. D., Bonewald, L. F., and White, K. E. (2006) *Nat. Genet.* **38,** 1310–1315
24. Ravindran, S., Grys, T. E., Welch, R. A., Schapira, M., and Patston, P. A. (2004) *Thromb. Haemost.* **92,** 1277–1283
25. Ravindran, S., Narayanan, K., Eapen, A. S., Hao, J., Ramachandran, A., Blond, S., and George, A. (2008) *J. Biol. Chem.* **283,** 29658–29670
26. Stan, R. V., Roberts, W. G., Predescu, D., Ihida, K., Saucan, L., Ghitescu, L., and Palade, G. E. (1997) *Mol. Biol. Cell* **8,** 595–605
27. Lamb, H. K., Mee, C., Xu, W., Liu, L., Blond, S., Cooper, A., Charles, I. G., and Hawkins, A. R. (2006) *J. Biol. Chem.* **281,** 8796–8805
28. Chen, S., Rani, S., Wu, Y., Unterbrink, A., Gu, T. T., Gluhak-Heinrich, J., Chuang, H. H., and Macdougall, M. (2005) *J. Biol. Chem.* **280,** 29717–29727
29. Marín-Briggiler, C. I., González-Echeverría, M. F., Munuce, M. J., Ghersevich, S., Caille, A. M., Hellman, U., Corrigall, V. M., and Vazquez-Levin, M. H. (2010) *Fertil. Steril.* **93,** 1574–1584
30. Hayakawa, K., Hiramatsu, N., Okamura, M., Yamazaki, H., Nakajima, S., Yao, J., Paton, A. W., Paton, J. C., and Kitamura, M. (2009) *J. Immunol.* **182,** 1182–1191
31. Chessler, S. D., and Byers, P. H. (1993) *J. Biol. Chem.* **268,** 18226–18233
32. Nandan, D., Ball, E. H., and Sanwal, B. D. (1990) *Biochem. Cell Biol.* **68,** 1057–1061